



ELSEVIER

Precambrian Research 100 (2000) 313–334

**Precambrian  
Research**

www.elsevier.com/locate/precamres

# A high-quality mid-Neoproterozoic paleomagnetic pole from South China, with implications for ice ages and the breakup configuration of Rodinia

David A.D. Evans<sup>a,\*</sup>, Z.X. Li<sup>b</sup>, Joseph L. Kirschvink<sup>a</sup>, Michael T.D. Wingate<sup>b</sup><sup>a</sup> *Division of Geological and Planetary Sciences, California Institute of Technology, Pasadena, CA 91125, USA*<sup>b</sup> *Tectonics Special Research Centre, The University of Western Australia, Nedlands, WA 6907, Australia*

## Abstract

Neoproterozoic (Sinian) sediments are exceptionally well preserved in the Three Gorges region (western Hubei Province) of the South China block. We report new paleomagnetic results, obtained independently by two separate laboratories, from a total of 157 samples of the  $748 \pm 12$  Ma, basal Sinian Liantuo Formation at its type locality. Detailed thermal demagnetization procedures and least-squares line analyses reveal three distinct magnetic components among the suite of samples. Two overprint components can be distinguished from each other by their laboratory unblocking temperatures. The first to be removed ('C'), always annihilated below  $600^\circ\text{C}$ , is common throughout the dataset but is amenable to least-squares line-fitting in only 37 samples. It yields a pole which in present coordinates resembles Mesozoic overprints identified from previous studies in the Three Gorges region ( $75.7^\circ\text{N}$ ,  $174.3^\circ\text{E}$ ,  $d_p = 6.0^\circ$ ,  $d_m = 8.3^\circ$ ,  $Q = 4$ ). The higher unblocking-temperature overprint ('B'), always subsidiary to the 'A' component, is more prevalent than 'C' and was identified by line-fitting in 67 samples. The 'B' direction is very steep and generates a paleopole whose in situ coordinates do not resemble the Mesozoic–Cenozoic apparent polar wander path for South China, and whose tilt-corrected coordinates ( $20.3^\circ\text{N}$ ,  $106.2^\circ\text{E}$ ,  $d_p = 7.2^\circ$ ,  $d_m = 7.3^\circ$ ,  $Q = 5$ ) bear no resemblance to any reliable Phanerozoic paleopoles from the South China block. The steep 'B' direction, if an unbiased representative of an ancient geomagnetic dipole field, was probably acquired some time in the 200 m.y. interval between deposition of the Liantuo Formation at  $\sim 750$  Ma and Cambrian time. The most stable component is a two-polarity remanence, removed at temperatures predominantly  $> 630^\circ\text{C}$ , which we infer to reside in hematite. A change in polarity of this component occupies a similar stratigraphic position (within 5 cm) among three outcrops separated by  $\sim 100$  m lateral distance. We calculate a mean paleomagnetic pole from each of the laboratories' datasets and combine these with a previously determined pole from correlative rocks in Yunnan [ $^{\circ}\text{N}1$ ' of Zhang and Piper, *Precambrian Res.* 85 (1997) 173–199], to obtain an overall weighted mean paleomagnetic pole ( $04.4^\circ\text{N}$ ,  $161.1^\circ\text{E}$ ,  $A_{95} = 12.9^\circ$ ,  $Q = 7$ ) for the South China block at  $748 \pm 12$  Ma. The combined 'Z1' pole is considered to be primary based on its thermal stability, its magnetostratigraphic consistency, and a soft-sediment fold test determined by previous work. Results from individual sampling areas constrain the depositional paleolatitude of the Liantuo Formation and equivalent Sinian rocks to  $30$ – $40^\circ$ . This result applies to one or both of the stratigraphically adjacent Chang'an and Nantuo glacial deposits; unfortunately, it is neither high nor low enough to refute any of the conceptual models for the enigmatic Neoproterozoic glaciations. The new basal Sinian paleopole, in the context of recent paleomagnetic and geochronological results from Australia, suggests that the Nantuo glaciation is pre-Marinoan. The new 'Z1' pole may also provide constraints on

\* Corresponding author. Present address: Tectonics Special Research Centre, The University of Western Australia, Nedlands, WA 6907, Australia.

E-mail address: devans@tsrc.uwa.edu.au (D.A.D. Evans)

the various proposed reconstructions of South China's position in Rodinia. In particular, a paleoposition adjacent to northwestern Australia at  $\sim 750$  Ma requires a specific relative orientation between the two blocks. Likewise, if Rodinia were still intact by 750 Ma, South China may have lain between Australia and Laurentia only in an orientation different from that originally proposed in the 'missing link' hypothesis. As a final alternative, the new paleomagnetic data could be used to position South China, Australia, and Laurentia in an immediately post-Rodinian paleogeography around the nascent Pacific Ocean. © 2000 Elsevier Science B.V. All rights reserved.

**Keywords:** Glaciation; Paleomagnetism; Proterozoic; Rodinia; Sinian; South China block

## 1. Introduction

Sub-Cambrian, unmetamorphosed, stratified rocks are widespread throughout China (Grabau, 1922). Grouped into the Sinian System, the deposits occur both north and south of the Qinling–Dabie Mountains (Wang, 1986), which contain the Mesozoic suture between the North China and South China blocks (Klimetz, 1983; Enkin et al., 1992). In the South China block (SCB), Sinian strata occur among several provinces; the type section is in the lower of the Three Gorges of the

Yangtze River. There, a structural dome affecting all pre-Cretaceous units and therefore related to the so-called Indosinian orogeny during late Mesozoic time, exposes the regional stratigraphy in 'onion-skin' fashion around the Huangling dome (Fig. 1). Pre-Sinian basement in the core of this feature consists of the Huangling batholith intruding Archean to Paleoproterozoic crystalline rocks (Wang et al., 1996). A phase of the batholith that nonconformably underlies Sinian strata has been dated by the SHRIMP U–Pb method on zircon at  $819 \pm 7$  Ma (Ma et al., 1984).

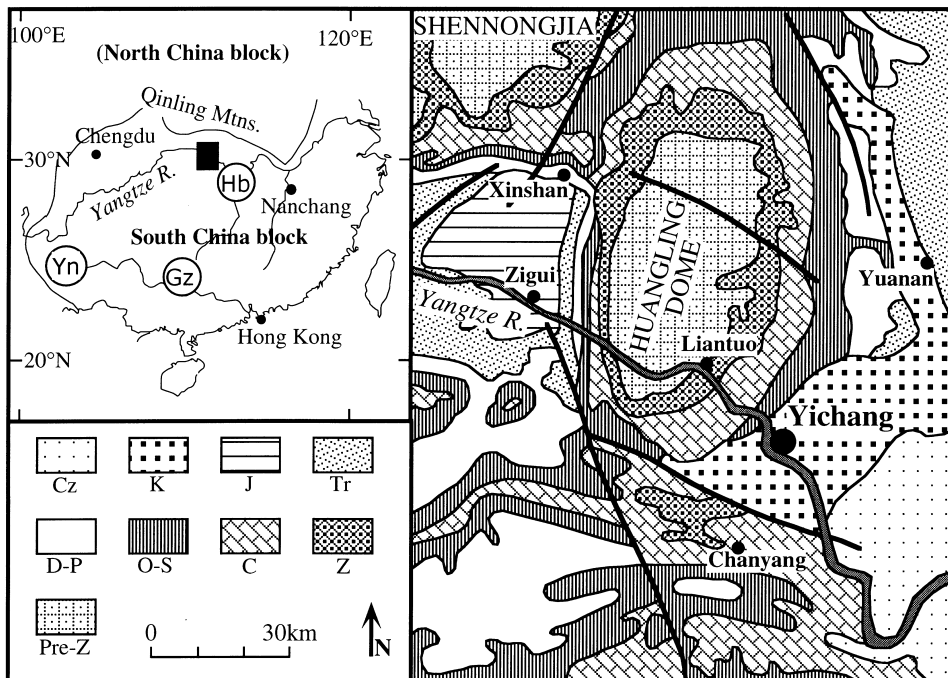


Fig. 1. Geology of the lower Three Gorges of the Yangtze River, after Wang et al. (1996). Liantuo village is located at ( $30^{\circ}51'N$ ,  $111^{\circ}09'E$ ); Yichang city at ( $30^{\circ}42'N$ ,  $111^{\circ}19'E$ ). Provinces: Yn=Yunnan, Hb=Hubei, Gz=Guizhou. Rock ages: Z=Sinian, C=Cambrian, O-S=Ordovician and Silurian, D-P=Devonian through Permian, Tr=Triassic, J=Jurassic, K=Cretaceous, Cz=Cenozoic. Dark lines are faults.

The basal Sinian, arkosic to argillitic Liantuo Formation contains interbedded volcanic ash horizons, one of which was dated at  $748 \pm 12$  Ma (Ma et al., 1984). Overlying the Liantuo Formation with apparent disconformity, the Nantuo Formation is the classic Sinian 'tillite'; it actually spans a range of glacial-sedimentary facies throughout the SCB (Wang et al., 1981; Liao, 1981). The Doushantuo Formation, primarily muddy dolostone with minor shale and bedded or nodular chert, is apparently disconformable upon the Nantuo diamictites when viewed at the regional level. It contains the Miaohe biota of Ediacaran or perhaps pre-Ediacaran age (Ding et al., 1996), and passes upward into the Dengying Formation bearing Ediacaran fauna, Vendotaenids, and in its upper member, small skeletal fossils marking the lowermost Cambrian (Wang et al., 1996; Fig. 2).

The Sinian has been interpreted as part of a continental-rift succession with subsequent passive-margin development, similar in style and age to those found in Australia and western North America. For this reason as well as others, Li et al.

(1995) reconstructed the SCB as the 'missing link' between Australia and Laurentia in the SWEAT configuration (Eisbacher, 1985; Bell and Jefferson, 1987; Moores, 1991), in the context of fragmentation of Rodinia (Powell et al., 1993; Li et al., 1996). Alternative reconstructions place South China adjacent to the northwest Australian shelf (e.g. Kirschvink, 1992a). We report new paleomagnetic data from the basal Sinian Liantuo Formation in South China, in order to constrain the paleogeography of Rodinia during its fragmentation. In addition, our work contributes one more datum to help define the spatial distribution of the widespread Neoproterozoic glacial deposits, the subject of a long-standing debate (Harland, 1964; Schermerhorn, 1974; Williams, 1975; Crowell, 1983; Hambrey and Harland, 1985; Embleton and Williams, 1986; Kirschvink, 1992b; Meert and Van der Voo, 1994; Williams et al., 1995; Evans, 1997, 1998; Hoffman et al., 1998).

Early paleomagnetic studies of the basal Sinian sedimentary rocks in the Yangtze Gorges region and correlative strata within the SCB found only a high-paleolatitude direction (Liu and Liu, 1965) that was stable to alternating-field demagnetization (Liu and Feng, 1965) and verified by subsequent workers (Li and Liu, 1979). At the time, the results were welcomed as being consistent with the lower Sinian glacial record, but in hindsight we regard those early studies as inadequate by today's paleomagnetic standards. A dramatically different paleomagnetic result from the Liantuo Formation in the type area, indicating low paleolatitudes, was obtained by Zhang et al. (1982) (summarized in Zhang and Zhang, 1985). As these data were also obtained only by alternating-field demagnetization, it is unlikely that the hematitic components (see below) of the Liantuo redbeds were separated completely. Further study, using the more appropriate techniques of thermal demagnetization and least-squares analysis (Kirschvink, 1980), on correlative basal Sinian rocks located  $\sim 150$  km east of the Three Gorges region, revealed a near-equatorial paleolatitude (Zhang et al., 1991). Even farther east, in the so-called Jiangnan terrane, correlative basal Sinian volcanic and sedimentary rocks again yielded a near-equatorial paleolatitude, but  $\sim 90^\circ$  different in azimuth from the previous

|            |                                 |            |  |
|------------|---------------------------------|------------|--|
| Camb.      |                                 |            | Dolostone, P-bearing                     |
| Sinian (Z) | Dengying Fm.                    |            | Dolostone with bedded chert and nodules  |
|            |                                 |            | Limestone, partly siliceous              |
|            |                                 |            | Oolitic dolostone                        |
|            |                                 |            | Dolostone intercalated with black shale  |
|            | Doushantuo Fm.                  |            |  |
| Sinian (Z) | Nantuo Fm.                      |            | "Tillite" (diamictite)                   |
|            | upper Liantuo Fm. $748 \pm 12$  | UWA<br>CIT | Mudstone interbedded with nonwelded tuff |
|            | lower Liantuo                   |            | Arkosic sandstone                        |
| pre-Z      | Huanglingmiao Suite $819 \pm 7$ |            | Trondjhemite, granodiorite               |

Fig. 2. Generalized Sinian stratigraphy in the Liantuo area, after Wang et al. (1996). SHRIMP U–Pb isotopic ages (in Ma) from Ma et al. (1984). Stratigraphic thicknesses are only approximate. Dark vertical bars denote the 'CIT' and 'UWA' sampled stratigraphic levels.

result (Zhang, 1998). These latter studies still fail to document their results completely, so it is difficult to judge their reliability; for example, the Zhang (1998) paper describes a positive fold test for the Liantuo-equivalent data, but the bedding corrections graphically shown in his fig. A1 are inconsistent with the stated bedding attitudes in table A2. Finally, another working group visited basal Sinian sedimentary rocks in the Yunnan Province of southwestern China and obtained a moderate paleolatitude (Zhang and Piper, 1997), the details of which will be discussed below.

## 2. Paleomagnetic field and laboratory methods

This paper is a combined report of two independent paleomagnetic studies of the Liantuo Formation, using different field strategies, laboratory instruments, and preferences of data analysis. As will be shown below, the paleomagnetic poles derived from the two laboratories are statistically distinguishable (by a few degrees), despite sampling within the same small area of the Yangtze River. For these reasons, we prefer to present our methods and results separately, combining them only at the end of the discussion. Hereafter, samples analyzed at the California Institute of Technology will be named 'CIT', whereas those analyzed at the University of Western Australia will be denoted 'UWA'.

As for the CIT samples, reconnaissance paleomagnetic work in 1986 led to the first collection of 40 cores obtained by portable drill from the upper part of the upper Liantuo Formation, exposed in the hills above Liantuo village at (30°51'N, 111°09'E). All cores were oriented with a magnetic compass, and solar-compass measurements for some samples demonstrated consistency of the magnetic deviation in the area. Laboratory analyses of these specimens in 1995 and early 1996 revealed a change in magnetic polarity at one level within the stratigraphic section. The second sampling trip to the Three Gorges in 1996, returning 103 drilled samples, was devoted primarily toward an attempt to reproduce the polarity zonation in an independent section of the same lithostratigraphic interval, as well as perhaps to obtain

transitional directions from within a Precambrian geomagnetic reversal. Sampling in the zone of the estimated polarity change was concentrated at 2–3 cm of stratigraphic spacing, near the limit of resolution using standard portable drilling techniques, as well as the limit in uncertainties of lithostratigraphic correlation of individual beds over lateral distances of decameters to hectometers. The stratigraphic distribution of paleomagnetic samples from this study is shown in Fig. 3. Most of the samples are purple–red mudstone, siltstone, or fine sandstone; some specimens include green mottling which generally follows certain layers but also cuts across bedding in many places. Based on field evidence alone, the green coloration is interpreted to indicate the flow of chemically reducing fluids through the rocks at some unknown time after deposition.

The CIT samples were trimmed to right-cylindrical specimens of 2.3 cm height, commonly yielding more than one specimen per sample, but only one being analyzed thus far. Laboratory analysis involved a SQUID cryogenic magnetometer and an automatic sample-changing system allowing as many as 400 consecutive, unaided measurements at each demagnetization step. For the 1986 samples, measurement of natural remanent magnetization (NRM) was followed first by alternating-field demagnetization at 2.5, 5.0, 7.5, and 10.0 mT, and then by thermal demagnetization (1 h at peak temperature) at 150, 250, 350, 450, 500, 550, 600, 630, 650, 660, 667, 672, 675, 678, and 682°C. For the 1996 samples, the steps were NRM; 5.0, 10.0, and 15.0 mT; and 250, 450, 570, 630, 650, 660, 667, 672, 676, 680, and 683°C. All 143 specimens received the full treatment of demagnetization steps, until their directional behavior became unstable due to acquisition of spurious magnetizations. Some specimens showed oscillatory demagnetization trajectories at temperatures greater than 650°C. Because the samples were placed in the oven in opposite orientations during alternating temperature steps, we suspect that these patterns result from partial-thermoviscous remanent magnetizations (pTVRM) acquired in the furnace, despite maintenance of ~30 nT or lower field strength throughout the heating chamber and less than 10 nT in the cooling chamber. To be certain

1986 Sampling

1996 Sampling

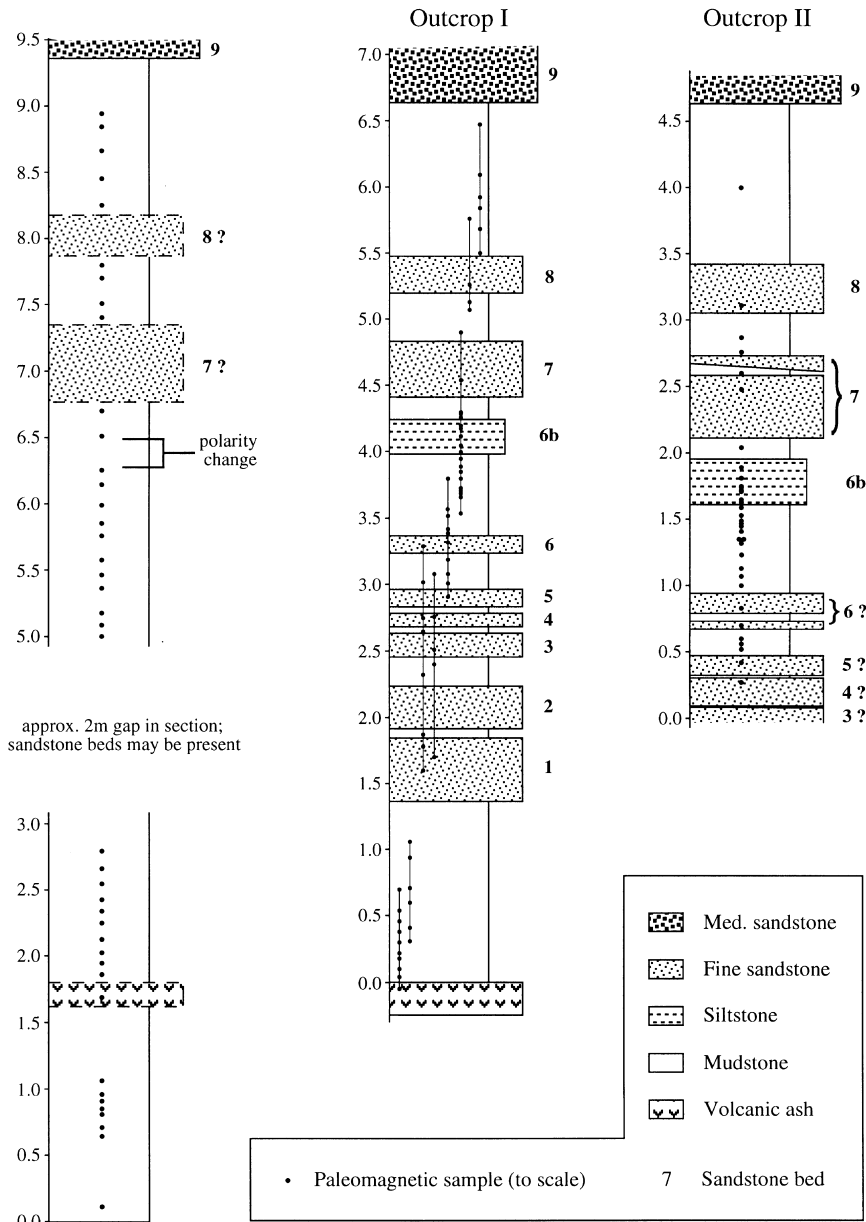


Fig. 3. Stratigraphic variation of 'CIT' samples from the upper Liantuo Formation. Solid dots represent the stratigraphic positions (in meters above arbitrary baselines) of 2.5 cm diameter paleomagnetic cores, drawn to scale. Individual sandstone/siltstone beds from outcrop I are numbered. The existence of sandstone beds at 7.0 and 8.0 m within the 1986-sampled section is only inferred from abnormally large stratigraphic intervals between samples at those levels. Sandstone bed #9, however, is unambiguously correlated among the three sections. Vertical lines connecting samples in outcrop I represent vertically aligned sample profiles, separated laterally from one another by approximately 5 m.

that no more information remained in the samples, some were demagnetized at additional thermal steps of 686, 690, and 695°C. Surprisingly, some specimens retained stable behavior even to these high temperatures, a pattern also reported in the study of correlative strata in Yunnan (Zhang and Piper, 1997). The majority of specimens from our study retained useful information to 675 or 680°C. In most cases, thermal unblocking spectra of the individual components did not overlap, permitting line-fitting by least-squares analysis (Kirschvink, 1980).

The 14 UWA samples were collected in 1993 by portable drill from two sites: one within Liantuo village in the lower part of the upper Liantuo Formation (Site 1); and the other in the hills, in the uppermost part of the upper Liantuo Formation, stratigraphically within 1 m of the overlying Nantuo 'tillite' (Site 2). The UWA sites thus 'straddle' the CIT outcrops stratigraphically (Fig. 2). Despite post-1993 construction of the wide access road to the Three Gorges Dam project that has obscured or destroyed the UWA sample sites, we estimate that all of the CIT and UWA sample localities lie within an area of  $\sim 1$  km<sup>2</sup>. Like the CIT collection, the UWA samples comprise fine-grained sandstone and siltstone. Right-cylindrical specimens of 2.2 cm height were trimmed from the cores, and analyzed using a SQUID cryogenic magnetometer. After measurement of NRM, all 14 specimens were subjected to thermal demagnetization steps of 100, 200, 300, 400, 500, 550, 600, 630, 650, 670, and 680°C. Linear magnetic components were identified via least-squares analysis (Kirschvink, 1980).

### 3. Directional data

From the CIT samples, three distinct magnetic components were identified by their directional groupings and thermal unblocking spectra (Figs. 4 and 5). Of these, the most stable component (labeled 'A') yielded the two polarities (west-up and east-down in present coordinates) that we identified from the year 1986 collection (Fig. 3), and that we subsequently tested for stratigraphic consistency. In order to understand the factors

contributing to the directional groupings of the three components, and to facilitate a reversals test on component 'A', results from the two polarity zones are discussed separately below.

From the lower polarity zone, where component 'A' is westward and upward in present coordinates [Fig. 5(a)], two additional components are observed overprinting 'A'. Fig. 4 shows typical demagnetization behavior among three subgroups of specimens, representing a total of 91 out of 99 samples. The subgroups are distinguished by the relative strength of the NRM held by the various components. The first subgroup [Fig. 4(a)] shows single-component behavior with only 'A' present, or perhaps an ill-defined and small northward and downward component removed by the alternating-field and low thermal steps. The second subgroup [Fig. 4(b) and (c)] includes the greatest number of samples and is characterized by subequal magnetizations of 'A' and an overprint component (usually 'C', rarely 'B'). Fig. 4(c) shows one of the few samples containing distinct and linear trajectories of all three components. The third subgroup [Fig. 4(d)] contains samples whose NRM is dominated by an overprint direction (usually 'B', rarely 'B' and 'C', in two samples only 'C'). For most samples within this subgroup, the 'A' component is recognizable only by great-circle trajectories toward west-up on the stereonet; these data are amenable to polarity interpretation but not least-squares line-fitting. In some cases, however, a stable endpoint is reached with linear decay toward the origin [e.g. Fig. 4(d)]. In four of the eight samples not included in the three subgroups, the polarity of the 'A' component is recognizable through great-circle analysis. Fig. 5(a) shows the distribution of 'A' among 69 least-squares lines whose mean angular deviation values (Kirschvink, 1980) are less than 10°.

Components 'B' and 'C' are distinguished by their thermal unblocking spectra: 'C' is always completely removed by 600°C, whereas 'B' is not. This criterion separates the overprint directions neatly into two Fisherian or circularly symmetric datasets [Fig. 5(b) and (c)]. As stated above, 'C' generally occurs equal in magnitude to 'A', whereas 'B', when present, tends to dominate the NRM. Although no trends are obvious when comparing

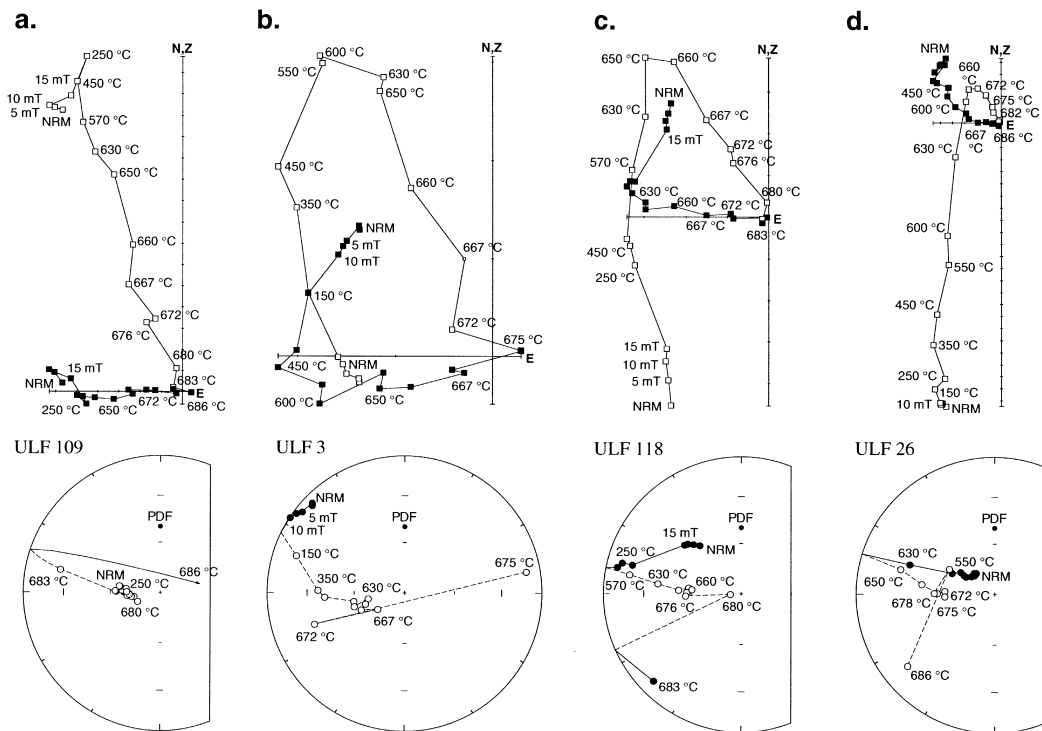


Fig. 4. Typical demagnetization trajectories, in present coordinates, of Liantuo mudstones from the lower polarity zone ('CIT' subset). Upper panels are superimposed-orthogonal-projection diagrams of measurements after the natural remanent magnetization (NRM) and subsequent partial demagnetization steps, with solid symbols in the horizontal plane and open symbols in the N–S vertical plane. Tick marks are at intervals of  $10^{-8} \text{ A m}^2$ . Lower panels are equal-area projections of the same data (symbols as in Fig. 5). (a) Single-component ('A') behavior representative of 22 samples. (b, c) Two components with equivalent vectorial lengths of magnetization, representative of 46 samples. In panel (b), component 'C' overprints 'A'; in panel (c), all three components are identifiable. (d) Overprint-dominated magnetization representing 23 samples. In this case, 'B' overprints 'A'.

sample coloration to demagnetization behavior, it should be noted that much of the green mottling affecting the section occurs in strata within the lower polarity zone; as will be demonstrated below, 'C' is largely absent from the upper polarity zone. This pattern, combined with the entirely sub- $600^\circ\text{C}$  unblocking spectrum for 'C', suggests that the magnetic carrier of that component is magnetite formed by chemical reduction via secondary fluid percolation through the section.

Components 'B' and 'A', with unblocking spectra ranging above  $600^\circ\text{C}$ , are likely carried by hematite. Ferromagnetic remanence in this mineral can arise from a number of depositional and post-depositional processes (Butler, 1992, pp. 197–203), and stability of thermal unblocking in the laboratory does not necessarily correspond to age of

remance acquisition. Therefore, from the preceding discussion alone, there is no compelling reason to accept 'A' as the primary magnetic component, despite its universally higher stability than 'B' and narrow thermal unblocking spectrum near the  $675^\circ\text{C}$  Néel temperature of hematite. Stratigraphic consistency of the two polarities in 'A', however, would strongly suggest that it is primary and 'B' secondary (see below).

Within the 44 samples from the upper polarity zone, two subgroups are identified (Fig. 6). In all 29 samples of the first subgroup, 'B' and the eastward-downward polarity of 'A' are identifiable and clearly distinguishable in both superimposed-orthogonal-projection diagrams and the equal-area stereonets [Fig. 6(a)]. In the second subgroup, the two components are not easily identified because

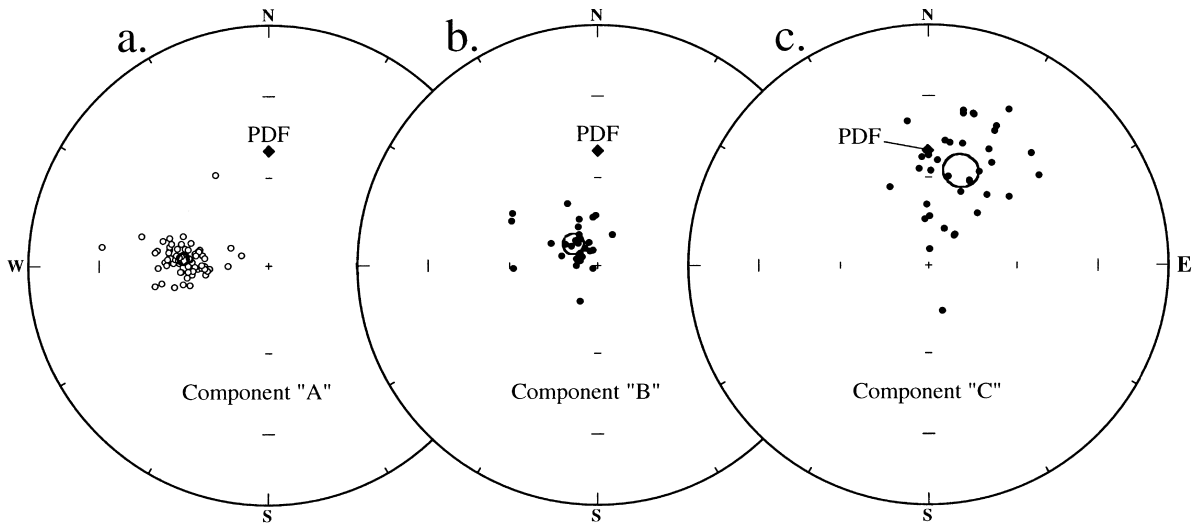


Fig. 5. Equal-area projections of least-squares line-fitted component vectors from the lower polarity zone ('CIT' subset), in present coordinates. Open (solid) symbols represent data from the upper (lower) hemisphere. The large ellipses are projections of the 95% confidence cones around the Fisher means. PDF = present geocentric axial dipole field direction at the sampling site. (a) Component 'A'. Nine samples have been excluded from this population because of mean-angular-deviation values greater than  $10^\circ$ . (b) Component 'B'. (c) Component 'C'.

a stable endpoint 'A' direction is not attained. In half of these samples, component 'B' can be least-squares line-fitted, whereas only the polarity of 'A' is identifiable by great-circle migration away from the 'B' direction on the stereonet [Fig. 6(b)]. A component similar to 'C' from the lower polarity zone is largely absent, insignificant, or non-linear in samples from the upper polarity zone. As discussed above, 'C' may be related to localized chemical reduction and such greenish mottling is not prevalent in the upper polarity zone.

For all of the upper-polarity-zone samples, the straightest segments of the demagnetization trajectories were chosen without regard to unblocking temperature. Like the analysis for the lower polarity zone, mean-angular-deviation values greater than  $10^\circ$  were excluded from final statistical compilation. Nevertheless, the distribution of components 'A' and 'B' from the upper polarity zone is streaked (Fig. 7) and appears to define a mixing plane between two endmembers. The elongate distribution may be attributed to slightly overlapping thermal unblocking spectra between the two components within individual specimens; whereas

the overlap could easily be identified and avoided in samples of the lower polarity zone because of the  $\sim 150^\circ$  inter-component angle, in the upper polarity zone 'A' and 'B' are separated by only  $\sim 30^\circ$ , allowing some contamination of the overlapped part of the unblocking spectrum into the least-squares line analysis.

Both means for our components 'A' and 'B' from the upper polarity zone are displaced toward the centroid of the combined dataset (Fig. 7). This incomplete separation of the two components renders both a failed common mean test for 'B' and a failed reversals test for 'A' (bootstrap tests adapted from McFadden and McElhinny, 1990) at both 95% and 99% levels, between the two polarity zones. Despite this negative statistical result, we emphasize that the difference in means between upper and lower polarity zones is not great (e.g. less than  $5^\circ$  for component 'A'; Fig. 7), and that directions from the upper polarity zone should be included somehow in the calculation of our mean direction. To accomplish this, we find least-squares plane fits to the combined 'A' and 'B' components of all specimens from the upper

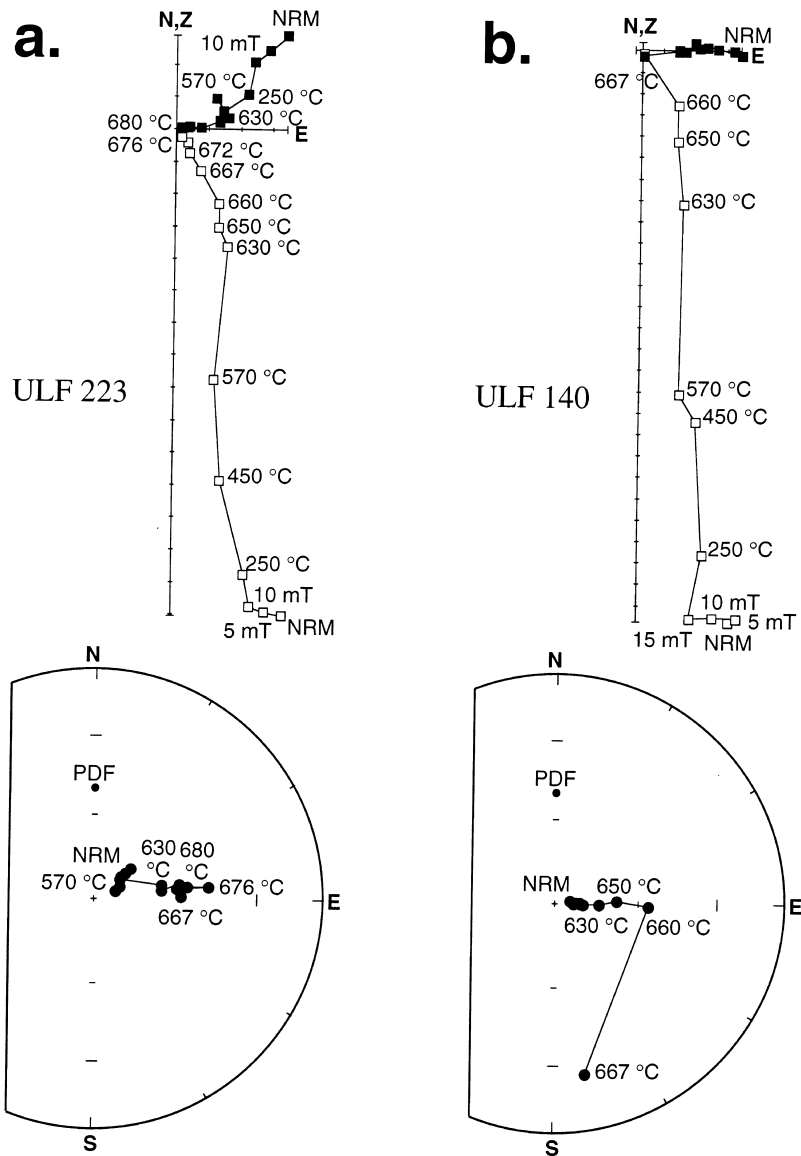


Fig. 6. Typical demagnetization trajectories, in present coordinates, of Liantuo mudstones from the upper polarity zone ('CIT' subset). Symbols as in Fig. 4. (a) Components 'A' and 'B' relatively easy to separate, representative of 29 samples. In this case, component 'C' may be present at the early demagnetization steps, and components 'A' and 'B' are separated by the 630°C step. (b) Components 'A' and 'B' difficult to separate, as observed in 14 samples.

polarity zone (which in itself can be evaluated using Bingham statistics; Onstott, 1980). We then combine the linear and planar data (using sector constraints) from all 'A' components into a Fisher mean direction (McFadden and McElhinny, 1988)

that includes 106 samples from both polarities and generates our preferred 'A<sub>CIT</sub>' paleomagnetic pole for the CIT dataset [Table 1, Fig. 8(a)]. We note that the mean direction using both polarities lies within 0.5° of the mean determined only from the

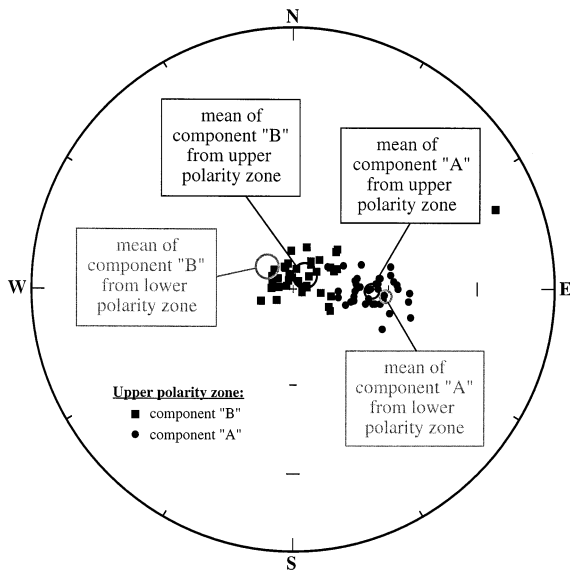


Fig. 7. Lower-hemisphere equal-area plot of overprint 'B' (squares) and characteristic component 'A' (circles) from the upper polarity zone ('CIT' subset), in present coordinates. Large ellipses are projections of 95% confidence cones about the means of components 'A' and 'B'; for comparison, Fisher means from the lower polarity zone ('A' inverted) are shown in gray.

lower polarity zone (Table 1), strongly suggesting internal concordancy within our combined 'CIT' dataset.

All of the 14 samples analyzed at UWA showed similar demagnetization behavior to that described above for the upper polarity zone, but apparently without any presence of a 'B' component. Component 'C' was generally of minor intensity, merely quasi-linear, and completely removed by 300°C. The 'A' component was identified by least-squares line analysis of only the highest (generally > 600°C) portion of each sample's demagnetization trajectory. Least-squares line analysis was performed on 13 of the 14 specimens; demagnetization of the remaining specimen revealed a trajectory toward the 'A' direction but lacking a stable endpoint. Mean directions from the two sites are not statistically different, so we consider the combined set in generating the 'A<sub>UWA</sub>' paleopole [Table 1, Fig. 8(b)].

#### 4. Magnetostratigraphy

The 'A' component is a highly stable, dual-polarity magnetic remanence identified cleanly in more than 75% of our samples. Stratigraphic variation in the 'A' remanence is also quite stable and consistent among the three CIT sections studied, where a single polarity switch is observed (Fig. 9). Following the results from the 1986 sample suite which originally identified the polarity change within a stratigraphic interval of ~20 cm, the two 1996 outcrops were sampled quite densely in that interval. The typical density of 2–3 cm between samples approaches the limit of resolution for the 2.5 cm diameter drilling apparatus, as well as the ~1 cm precision of stratigraphic measurements where limited outcrop availability may require as much as several meters of lateral distance separating stratigraphically adjacent samples.

Within the 1996 outcrops I and II, the polarity change occurs respectively within 41–46 cm and 40–46 cm below the base of sandstone bed #7. A more subtle lithological distinction appears approximately at this level in both sections: the base of a fine-grained siltstone unit (#6b in Fig. 3) similar in color to the mudstones but slightly more indurated (more noticeable as an increased resistance during drilling than any obvious macroscopic properties). The polarity change is coincident with the base of this unit in outcrop I, but approximately 5 cm above the base in outcrop II.

Several conceptual models can be put forward to try to explain these data. First, the 'A' component may be a two-polarity overprint acquired long after deposition and hence yielding no information regarding the depositional paleolatitude. If so, then that overprint would have migrated diachronously through the exposures over an interval of a few thousand years, the time considered to span a typical geomagnetic reversal. In doing so, it would have a sharply defined and remarkably consistent remagnetization 'front' maintaining a position 40–45 cm below sandstone bed #7. Neither a chemical (i.e. fluid-related) nor a thermal overprinting mechanism would be expected to maintain such stratigraphic regularity, for the flow paths of those sources would be expected to follow lithological boundaries between rocks of different

Table 1

Least-squares paleomagnetic directions from the Liantuo Formation, Three Gorges region (30.85°N, 111.15°E), South China

| Laboratory,<br>polarity zone/site | Component<br>(coordinate system) <sup>a</sup> | <i>n/N</i> | L/P | Fisher/Bingham statistics |              |                         |               |                       | Paleomagnetic pole |                |             |                       | Reliability           |         |          |
|-----------------------------------|---|------------|-----|---------------------------|--------------|-------------------------|---------------|-----------------------|--------------------|----------------|-------------|-----------------------|-----------------------|---------|----------|
|                                   |   |            |     | <i>D</i> (°)              | <i>I</i> (°) | <i>k/k</i> <sub>1</sub> | $\alpha_{95}$ | <i>k</i> <sub>2</sub> | $\alpha_{95}$      | $\lambda$ (°N) | $\phi$ (°E) | <i>d</i> <sub>p</sub> | <i>d</i> <sub>m</sub> | 1234567 | <i>Q</i> |
| CIT, Lower                        | 'A' (in situ)                                 | 69/99      | L   | 272.1                     | −61.0        | 82.0                    | 1.9           |                       |                    | 18.7           | 162.7       | 2.2                   | 2.9                   |         |          |
|                                   | (tilt-corrected)                              |            |     | 288.6                     | −53.2        | 82.4                    | 1.9           |                       |                    | 03.3           | 163.3       | 1.8                   | 2.6                   |         |          |
|                                   | 'B' (in situ)                                 | 29/99      | L   | 308.9                     | 79.0         | 57.5                    | 3.6           |                       |                    | 42.3           | 088.7       | 6.5                   | 6.8                   |         |          |
|                                   | (tilt-corrected)*                             |            |     | 203.8                     | 84.2         | 53.6                    | 3.7           |                       |                    | 20.3           | 106.2       | 7.2                   | 7.3                   | 1110101 | 5        |
| CIT, Upper                        | 'C' (in situ)*                                | 37/99      | L   | 015.9                     | 55.8         | 17.8                    | 5.8           |                       |                    | 75.7           | 174.3       | 6.0                   | 8.3                   | 1110100 | 4        |
|                                   | (tilt-corrected)                              |            |     | 034.7                     | 64.3         | 17.6                    | 5.8           |                       |                    | 59.2           | 161.6       | 7.4                   | 9.3                   |         |          |
|                                   | 'A' (in situ)                                 | 37/44      | L   | 088.9                     | 65.2         | 103.2                   | 2.3           |                       |                    | 22.8           | 158.6       | 3.0                   | 3.7                   |         |          |
|                                   | (tilt-corrected)                              |            |     | 108.8                     | 57.4         | 92.7                    | 2.5           |                       |                    | 05.6           | 159.7       | 2.7                   | 3.7                   |         |          |
| CIT, Total                        | 'B' (in situ)                                 | 38/44      | L   | 038.4                     | 84.3         | 37.6                    | 3.8           |                       |                    | 39.4           | 120.2       | 7.4                   | 7.5                   |         |          |
|                                   | (tilt-corrected)                              |            |     | 128.2                     | 77.8         | 35.3                    | 4.0           |                       |                    | 15.1           | 130.0       | 7.1                   | 7.5                   |         |          |
|                                   | A ⊙ B (in situ)                               | 37/44      | P   | 087.1                     | 68.8         | −88.2                   | 1.8           | −8.5                  | 7.5                | 25.6           | 153.9       | –                     | –                     |         |          |
|                                   | (tilt-corrected)                              |            |     | 110.7                     | 61.6         | −78.9                   | 1.9           | −8.5                  | 8.1                | 07.2           | 155.0       | –                     | –                     |         |          |
| UWA, Site 1                       | 'A' (in situ)                                 | 106/143    | L+P | 272.0                     | −60.7        | 61.1                    | 1.8           |                       |                    | 18.6           | 163.1       | 2.1                   | 2.7                   |         |          |
|                                   | (tilt-corrected)*                             |            |     | 288.3                     | −53.0        | 59.0                    | 1.8           |                       |                    | 03.4           | 163.6       | 2.1                   | 2.7                   | 1111111 | 7        |
| UWA, Site 2                       | 'A' (in situ)                                 | 6/7        | L   | 067.1                     | 65.6         | 71.4                    | 8.0           |                       |                    | 37.2           | 162.1       | 10.6                  | 13.0                  |         |          |
|                                   | (tilt-corrected)                              |            |     | 102.6                     | 60.9         | 71.4                    | 8.0           |                       |                    | 11.7           | 159.0       | 9.4                   | 12.2                  |         |          |
| UWA, Total                        | 'A' (in situ)                                 | 7/7        | L   | 065.9                     | 56.2         | 32.6                    | 10.7          |                       |                    | 36.0           | 175.8       | 11.1                  | 15.4                  |         |          |
|                                   | (tilt-corrected)                              |            |     | 091.7                     | 53.6         | 32.6                    | 10.7          |                       |                    | 15.5           | 170.3       | 10.4                  | 14.9                  |         |          |
| UWA, Total                        | 'A' (in situ)                                 | 13/14      | L   | 066.4                     | 60.6         | 40.4                    | 6.6           |                       |                    | 36.7           | 169.9       | 7.7                   | 10.1                  |         |          |
|                                   | (tilt-corrected)*                             |            |     | 096.2                     | 57.1         | 40.4                    | 6.6           |                       |                    | 13.9           | 165.3       | 7.0                   | 9.6                   | 1010101 | 4        |

<sup>a</sup> Abbreviations: \* Used for final calculation of paleopoles. ⊙ Conjunction of two linear components into planar analysis. *n/N*= number of samples used to compute mean/number measured; L=Fisher line analysis (Fisher, 1953); P=Bingham plane analysis (Onstott, 1980); L+P=combined line and plane analysis (McFadden and McElhinny, 1988); *D*=mean declination; *I*=mean inclination; *k*=best estimate of Fisher precision parameter; *k*<sub>1</sub>, *k*<sub>2</sub>=best estimates of Bingham precision parameters;  $\alpha_{95}$ =semi-radius (°) of 95% confidence cone;  $\lambda$ =paleopole latitude;  $\phi$ =paleopole longitude; *d*<sub>p</sub>, *d*<sub>m</sub>=lengths of minor and major semi-axes (°) of 95% confidence ellipse about paleopole; *Q*=reliability scale from Van der Voo (1990).

porosity or conductivity. The fact that 'A' polarities are consistent among both sandstone and mudstone in all three outcrops suggests that diachronous diffusive flow, either fluid or thermal, was *not* responsible for the polarity change.

Considering a geomagnetic polarity reversal occurring near the time of deposition, then it is difficult to determine whether the polarity change records the reversal in 'real-time' or whether there is a time lag of some sort, e.g. due to lithification processes. The range of timescales for magnetic remanence acquisition by hematite in redbeds is reviewed by Butler (1992, pp. 197–203) and is not easily determined in the laboratory. Note that from the two outcrops with detailed sampling, no transitional directions are observed between polarity zones; although somewhat erratic directional

behavior just below the polarity change can be observed in both outcrops I and II (Fig. 9), this is due to less linear demagnetization trajectories in these units rather than well-defined lines in unusual orientations, as might be expected from true transitional directions. The lack of transitional directions implies that either sedimentation was slow relative to the change in geomagnetic polarity during 'real-time' acquisition, or a post-depositional remanence due to dewatering or diagenesis obliterated any transitional remanence directions originally present.

Another possible model of immediate post-depositional remanence is that during the reversal Earth's field strength declined, causing the transitional directions to be of low ferromagnetic stability. As geomagnetic field strength rebounded

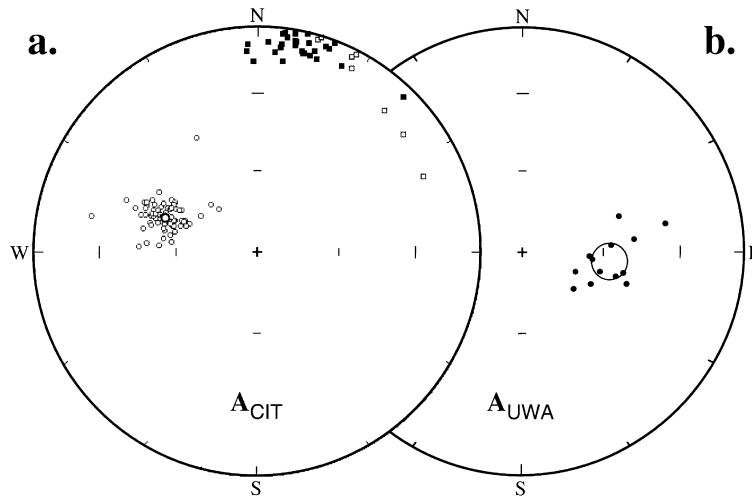


Fig. 8. Equal-area projections of the ‘A’ component in tilt-corrected coordinates. (a) ‘CIT’ subset; 106 samples from both polarity zones. Open (solid) symbols represent the upper (lower) hemisphere. Circles are least-squares lines from the lower polarity zone; squares are the poles to least-squares planes from the upper polarity zone. Dark ellipse is a projection of the 95% confidence cone about the Fisher mean of all samples. (b) ‘UWA’ subset; lower hemisphere. Large ellipse is a projection of the 95% confidence cone about the Fisher mean.

into the new polarity chron, unlithified sediments deposited during the transition became remagnetized with the new polarity. In these cases, the apparent reversal near the base of unit #6b may actually have occurred during deposition of, say, sandstone bed #7.

In the ‘real-time’ scenario, the 5 cm discordance between outcrops I and II of the polarity change relative to the base of unit #6b can be explained by an onlap relationship of the siltstone from outcrop II to outcrop I, whereby the base of unit #6b in outcrop I would represent a mild unconformity. Such an onlap gradient of 5 cm over a lateral distance of  $\sim 100$  m is plausible for the presumed fluvial–deltaic sedimentary environment of the upper Liantuo Formation, and in accordance with observed thickness variations of the lithological units (Fig. 3).

Because many of the sampled horizons are fine-grained mudstones, we explore the possibility that post-depositional compaction may have deflected (shallowed) the primary or earliest diagenetic ‘A’ remanence described above. If that were the case, then the observed magnetic inclination would be misconstrued to underestimate the true paleolatitude (because paleolatitude is directly related to

magnetic inclination according to the axial geocentric dipole hypothesis). Post-depositional compaction should have affected the mudstones more than the sandstones, and this can be tested within the large CIT dataset (using samples only from the non-biased lower polarity zone of the well-documented 1996 outcrops). Of the 12 fine-grained sandstone samples, mean tilt-corrected inclination is  $-55.2 \pm 4.0^\circ$ ; the 31 mudstone samples yield a mean inclination of  $-52.8 \pm 2.5^\circ$  (error bars taken from the  $\alpha_{95}$  of the respective means). These means are indistinguishable, supporting the notion that post-depositional sedimentary compaction has not substantially shallowed our primary ‘A’ component.

## 5. Paleomagnetic poles and ages

The ‘C’ pole associated with low thermal stability and secondary greenish coloration in the rocks is located prior to tilt-correction near previously determined Jurassic–Cretaceous poles from the SCB (and in fact all of China; Zhao et al., 1996). The location is near poles derived from a widespread overprinting episode affecting

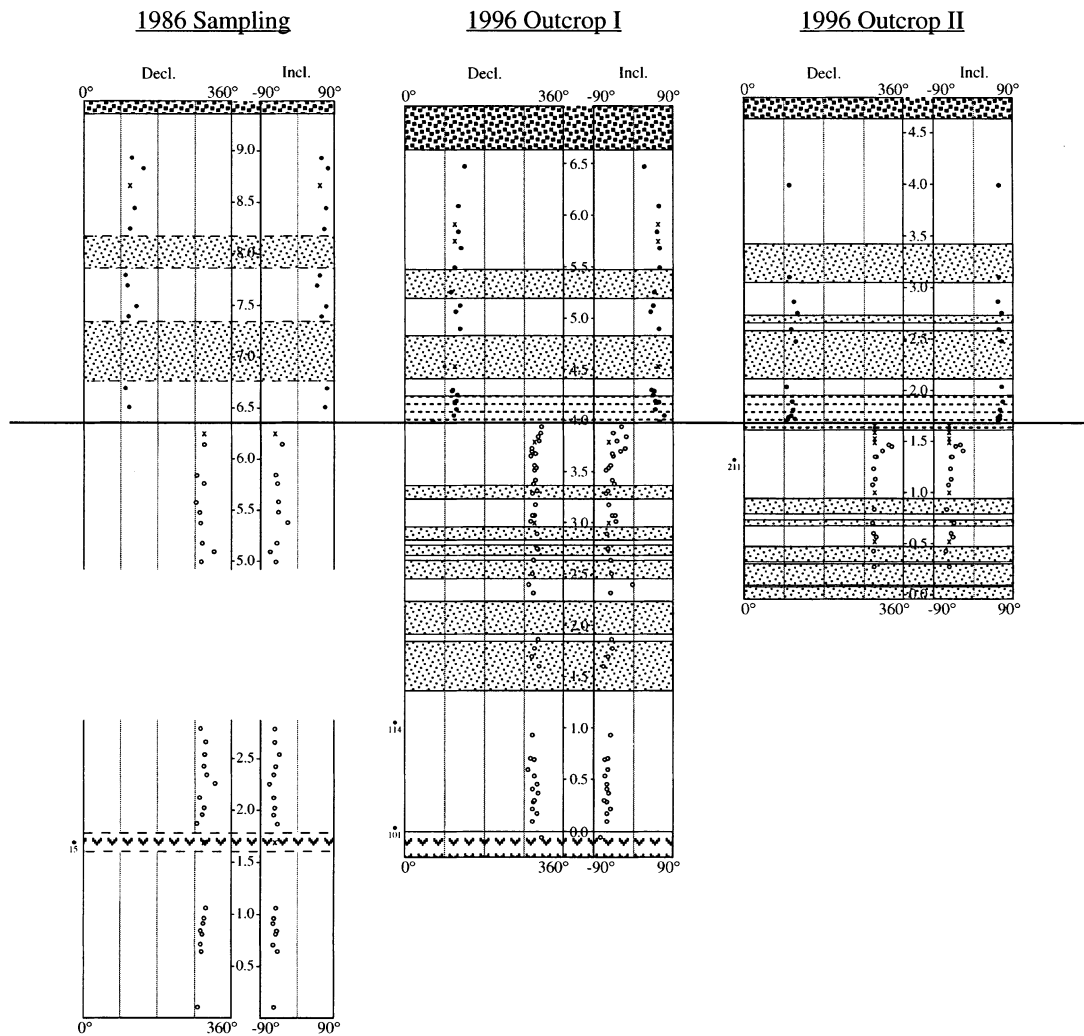


Fig. 9. Stratigraphic variation of component 'A' from the three sampled sections, showing declinations (left) and inclinations (right) in tilt-corrected coordinates. Lithological patterns as in Fig. 3. Stratigraphic height in meters, in the center of each column. Open (solid) circles depict least-squares line-fitted data from samples, approximately to scale, in the lower (upper) polarity zone. Samples not amenable to least-squares line-fitting, but whose polarity designations are obvious, are demarcated by 'x' at the mean direction. The four samples with no determinable polarity designation are labeled by sample number at the left side of the columns. The horizontal datum spanning the three sections denotes the level of change in polarity.

Paleozoic sedimentary rocks in the Three Gorges region (Kent et al., 1987), and distinct from the present rotation axis. Upon correction for the tilt of bedding, the 'C' pole becomes distinct from the existing group of late Mesozoic poles, suggesting that 'C' was acquired soon after Indosinian tilting, in Jurassic–Cretaceous time. The 'C' pole rates a four on the 'Q' scale of Van der Voo (1990),

lacking field stability tests and dual polarity, and showing similarity to late Mesozoic poles.

The 'B' pole, derived from the steep, hematite-borne overprint observed in both polarity zones, is far-removed from the majority of Cretaceous to Recent paleopoles from the SCB. A few examples of similar, anomalously steep directions have been described from the early studies of the Three

Gorges area (Liu and Liu, 1965; Liu and Feng, 1965; Li and Liu, 1979), as well as from more recent work in the eastern SCB on rocks as young as Carboniferous (Li, 1988, pp. 149–152) and Triassic (Opdyke et al., 1986). In both of those latter studies, the steep direction was determined to be post-folding (post-Jurassic), and conjectured to be possibly an artifactual resultant of two or more components with strongly overlapping demagnetization spectra. We consider this cause unlikely in our study, for the ‘B’ component constitutes well-defined, linear demagnetization segments, commonly dominating the NRM (Figs. 4 and 6). As another possibility, Opdyke et al. (1986) suggested that the steep direction may have been acquired along the axis of the cores during drilling. That possibility can be ruled out definitively in our study, for nearly all of the CIT samples were drilled subhorizontally into the outcrops. In any case, we believe that the steep, post-Jurassic magnetization rarely observed in previous studies does not indicate a polar position of the SCB during the last 150 Myr, and that the apparent polar wander path presented by Zhao et al. (1996; Fig. 10) is accurate to first-order for those times. Consequently, we consider the ‘B’ pole only in tilt-corrected coordinates, whereby it lies directly atop southern China.

Unfortunately, the age of this pole is not well-constrained. It is dissimilar to all previously reported Paleozoic poles, except for broad similarity to a pre-fold result from Early Ordovician sedimentary rocks in Yunnan (Fang et al., 1990; ‘O1’ in Fig. 10). This latter pole was discounted as anomalous by Zhao et al. (1996), but if it is in fact valid, then our component ‘B’ may have been acquired around Early Ordovician time. It should be cautioned, however, that the platform-carbonate-dominated succession throughout the early Paleozoic of southern China (Wang et al., 1996) would argue against such a high paleolatitude at that time.

Alternatively, the ‘B’ pole may be applicable to Sinian time, some time within the 200 m.y. interval between Liantuo deposition at  $748 \pm 12$  Ma and the Cambrian Period. A uniformitarian view of the latitudinal ranges of carbonate vs. glaciogenic sediment deposition would suggest that the ‘B’

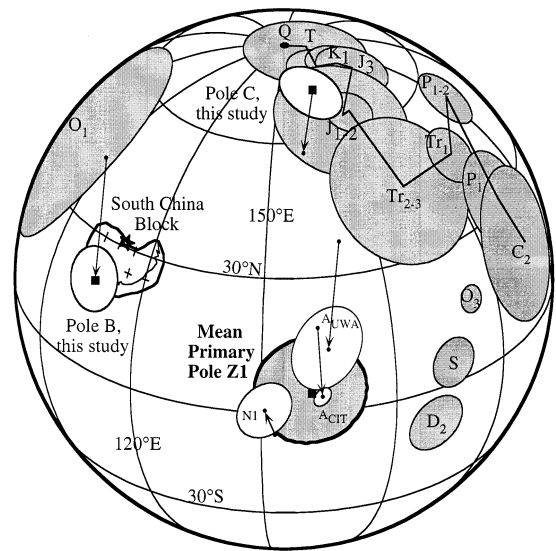


Fig. 10. Orthographic projection of paleomagnetic poles generated from components ‘A’, ‘B’, and ‘C’, relative to existing paleopoles from the South China block. The star indicates the Three Gorges region. Arrows denote the tilt correction upon paleopoles from this study, as well as pole ‘N1’ from the recent study of basal Sinian strata in Yunnan by Zhang and Piper (1997). The shaded and highlighted pole is the weighted-mean primary paleopole for the SCB at  $748 \pm 12$  Ma. Other shaded poles are from Phanerozoic rocks and summarized by Zhao et al. (1996). O<sub>1</sub> = Early Ordovician, O<sub>3</sub> = Late Ordovician, S = Silurian, D<sub>2</sub> = Middle Devonian, C<sub>2</sub> = Late Carboniferous, P<sub>1</sub> = Early Permian, P<sub>1-2</sub> = mid-Permian, Tr<sub>1</sub> = Early Triassic, Tr<sub>2-3</sub> = Middle–Late Triassic, J<sub>1-2</sub> = Early and Middle Jurassic, J<sub>3</sub> = Late Jurassic, K<sub>1</sub> = Early Cretaceous, T = Tertiary, and Q = Quaternary (present rotational axis).

component would have been acquired during the Nantuo ice age, whose deposits disconformably overlie the Liantuo Formation. This is inconsistent, however, with the results of Zhang and Piper (1997), which demonstrate consistency of their moderate-paleolatitude ‘A1’ remanence in both the Chengjiang (probably Liantuo equivalent) and the overlying Nantuo Formations. Furthermore, we note that strict uniformitarianism may not be applicable to Neoproterozoic paleoclimate, for at least one glacial deposit of that time period appears to have formed in cold conditions at sea-level, near the paleo-equator (Embleton and Williams, 1986; Sohl et al., 1999). Given these uncertainties, we interpret the ‘B’ pole — if truly representative of an ancient geomagnetic field — to be of Sinian

age, perhaps or perhaps not related to the latest stages of a diachronous Nantuo ice age. On the Van der Voo (1990) reliability scale, the 'B' pole rates a five, failing the categories of field stability tests and the presence of reversals.

Stratigraphic consistency of the polarity zones observed in three independently logged lithostratigraphic sections strongly suggests acquisition of magnetic component 'A' either concurrently with or shortly after deposition, spanning the time of a geomagnetic reversal. Polarity of component 'A' from the stratigraphically lowest 'UWA' site differs from the lowermost 'CIT' samples and suggests that our combined sample suite was drawn from at least three separate polarity chrons; therefore, our mean direction adequately averages secular variation of the geomagnetic field. Assuming that the axial geocentric dipole model holds true for mid-Neoproterozoic time (cf. Kent and Smethurst, 1998), the 'A' direction can provide constraints upon the depositional paleolatitude of the basal Sinian deposits and global paleogeography at  $748 \pm 12$  Ma.

We prefer to separate the 'CIT' and 'UWA' datasets even at the level of paleomagnetic pole generation, for several reasons. First, our mean directions are statistically distinct (Figs. 8 and 10). This discrepancy, we believe, is at least partly explained by the little-mentioned systematic biases inherent to paleomagnetic sampling, laboratory, and analytical methods (cf. the lucid description by Van der Voo, 1993, pp. 17–19). Second, we do not wish to lose this distinction between our two datasets when we average our results with others from the basal Sinian of the SCB (Zhang and Piper, 1997; see below). Third, separation of our datasets at the paleopole level and comparison with the Zhang and Piper (1997) result provides the minimum three determinations necessary to compute confidence limits on the overall mean paleopole.

The 'CIT' paleomagnetic pole is computed from tilt-corrected least-squares lines and planes of both polarity zones, to lie at ( $03.4^\circ\text{N}$ ,  $163.6^\circ\text{E}$ ), with 95% confidence-ellipse semi-axes of ( $d_p = 1.6^\circ$ ,  $d_m = 2.2^\circ$ ). Given that stratigraphically consistent polarity zonation among several outcrops at the cm-resolution constitutes an acceptable field

stability test, the 'A<sub>CIT</sub>' paleopole rates at  $Q=7$ , satisfying all of the criteria outlined by Van der Voo (1990). The 'UWA' dataset yields a tilt-corrected 'A<sub>UWA</sub>' paleopole at ( $13.9^\circ\text{N}$ ,  $165.3^\circ\text{E}$ ) with ( $d_p = 7.0^\circ$ ,  $d_m = 9.6^\circ$ ). This pole rates a four on the 'Q'-scale, with fewer than 25 samples, lack of a field stability test, and single polarity.

Our new paleomagnetic poles are similar to the 'N1' result reported recently by Zhang and Piper (1997) from basal Sinian sedimentary rocks in Yunnan, southwest China,  $\sim 1000$  km southwest of the Three Gorges region. That work involved pre-glacial, probably Liantuo-equivalent, strata of the Chengjiang Formation, as well as the overlying, syn- and post-glacial Nantuo Formation. They found a hematite-borne, high stability component that appears to be primary based on a soft-sediment fold test. The consistency of their result with ours suggests that to first-order the northwestern half of the South China block has remained structurally coherent, especially with regard to vertical-axis rotations, since Sinian time. Some minor vertical-axis rotations of a few degrees may have occurred during the gentle folding of the two regions, however, so we must combine the three basal Sinian paleopoles from the two regions in order to be confident that the resulting overall mean pole truly represents 'cratonic' South China. The three poles from the different laboratories cluster significantly better upon restoration of bedding, indicating a positive regional-scale fold test. Because the folding is predominantly Mesozoic, however, this fold test is not as useful as the other tests, described above, for demonstrating a primary 'A' magnetization in the sampled lower Sinian rocks. Note that our 'A' component somewhat resembles the direction obtained by Zhang et al. (1982), who used only alternating-field demagnetization on Liantuo-correlative strata in eastern Hubei. As their mean direction is significantly distinct from both our 'A' and 'B' directions, we suspect that the alternating-field technique failed to isolate the various magnetic components in that study; therefore, we omit that result from our overall mean pole calculation.

There are numerous ways to combine the three paleopoles; we desire a weighting scheme that adequately represents the uncertainties of the indi-

Table 2  
Weighted means of three lower Sinian paleomagnetic poles

| Weighting factor             | $A_{\text{CIT}}^{\text{a}}$ | $A_{\text{UWA}}^{\text{b}}$ | $N1^{\text{c}}$ | Total weight | Mean paleomagnetic pole |       |      |          |
|------------------------------|-----------------------------|-----------------------------|-----------------|--------------|-------------------------|-------|------|----------|
|                              |                             |                             |                 |              | (°N)                    | (°E)  | $K$  | $A_{95}$ |
| Uniform                      | 1                           | 1                           | 1               | 3            | 05.8                    | 160.0 | 59.8 | 16.1     |
| Regional                     | 0.750                       | 0.750                       | 1.500           | 3            | 04.4                    | 157.8 | 58.2 | 16.3     |
| $Q$ (normalized)             | 1.313                       | 0.750                       | 0.938           | 3            | 05.0                    | 160.1 | 67.8 | 15.1     |
| $N$ (normalized)             | 1.787                       | 0.219                       | 0.994           | 3            | 03.1                    | 159.6 | 94.3 | 12.8     |
| $k$ (normalized)             | 1.549                       | 1.060                       | 0.391           | 3            | 06.7                    | 162.5 | 89.0 | 13.1     |
| $1/\alpha_{95}$ (normalized) | 1.837                       | 0.501                       | 0.662           | 3            | 04.4                    | 161.1 | 91.8 | 12.9     |

<sup>a</sup> This study; pole (03.4°N, 163.6°E),  $Q=7$ ,  $N=106$ ,  $k=59$ ,  $\alpha_{95}=1.8^\circ$ .

<sup>b</sup> This study; pole (13.9°N, 165.3°E),  $Q=4$ ,  $N=13$ ,  $k=40.4$ ,  $\alpha_{95}=6.6^\circ$ .

<sup>c</sup> From Zhang and Piper (1997); pole (00.2°N, 151.2°E),  $Q=5$ ,  $N=59$ ,  $k=14.9$ ,  $\alpha_{95}=5.0^\circ$ .

vidual datasets. This is obviously a somewhat subjective exercise, so several alternatives are presented in Table 2. A requirement of all of the weighting schemes is that the total weight be normalized to the number of paleopoles; otherwise, the overall mean pole will bear fictitious precision. We prefer the ( $1/\alpha_{95}$ ) weighting factor because it incorporates individual pole precision in terms of both  $N$ , the number of samples analyzed, and  $k$ , the precision of each distribution. Note that all of the mean paleopoles generated by the various weighting factors lie within  $\sim 5^\circ$  of each other, well within their respective confidence cones (Table 2). Our preferred tilt-corrected mean paleomagnetic pole for the South China block at  $748 \pm 12$  Ma, which we name 'Z1' for its occurrence in lower Sinian (Z) rocks, is thus (04.4°N, 161.1°E,  $K=91.8$ ,  $A_{95}=12.9^\circ$ ,  $Q=7$ ).

## 6. Discussion

### 6.1. Implications for the Neoproterozoic ice ages

A primary age for the 'A' component allows us to constrain the depositional paleolatitude of the lower Sinian glaciogenic deposits. Because much of the uncertainty ( $A_{95}=12.9^\circ$ ) of the overall mean paleopole results from differences in declination that have no bearing on latitudinal estimates, we consider the paleolatitudes according to mean inclination values from each of the three studies.

Paleolatitudinal uncertainties for each dataset are computed from the 95% error limits on the mean inclination. Mean local paleolatitudes are thus  $33.6 \pm 1.7^\circ$  (CIT) and  $37.7 + 7.6 / - 6.5^\circ$  (UWA) from the Three Gorges region; and  $37.2 + 5.6 / - 5.0^\circ$  (Zhang and Piper, 1997) from Yunnan Province. These three estimates suggest moderate paleolatitudes (30–40°) for the basal Sinian deposits across the SCB. Note that if the combined dipole-octupole geomagnetic field model of Kent and Smethurst (1998) is correct for Sinian time, then these apparent paleolatitudes may underestimate the true paleolatitudes by  $\approx 15^\circ$ .

Although there exist several possibilities for correlating lower Sinian deposits across South China (Fig. 11), this should not affect the applicability of our Z1-derived paleolatitudes to the various glaciogenic deposits. According to Liao (1981) and Wang (1986), the glaciogenic Chang'an Formation exposed in the southeastern part of the SCB represents a significantly older glacial episode than the ubiquitous Nantuo glaciation [Fig. 11(a)]. Even so, the paleomagnetically sampled Liantuo Formation (this study) and Chengjiang/Nantuo Formations (Zhang and Piper, 1997) span the glaciogenic interval with consistently moderate paleolatitudes. Alternative correlations (Lu et al., 1985; Li et al., 1996; Li, 1998) include the Chang'an and Nantuo deposits within a single glacial interval separated by only a brief interglacial period [Fig. 11(b)]. In support for the latter model, the lithologically uncommon Mn- and

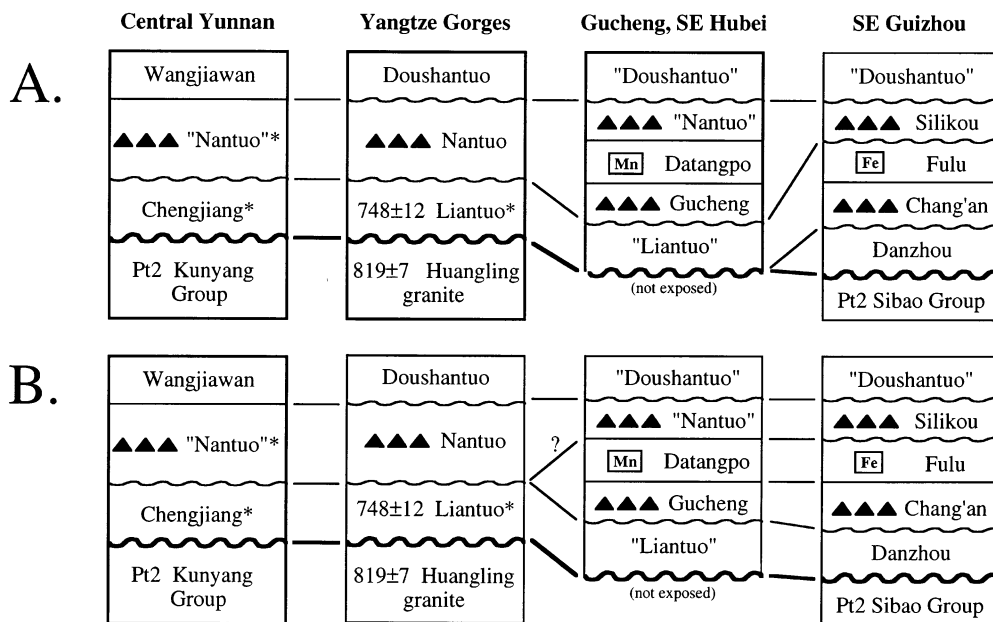


Fig. 11. Alternative correlation schemes for the Sinian of the South China block. Dark contacts depict profound stratigraphic breaks such as angular unconformities or nonconformities; light wavy curves show more subtle, regional disconformities; straight contacts are interpreted as conformable. Names enclosed by quotation marks indicate occurrences outside the type localities. Triangles represent glaciogenic deposits; 'Mn' and 'Fe' depict formations with bedded manganese and iron-formation, respectively. Pt2 = Mesoproterozoic. Asterisks mark the formations contributing to the combined paleomagnetic pole Z1. Ages in Ma (Ma et al., 1984; Li, 1998). (a) Correlation scheme of Liao (1981) and Wang (1986). (b) Alternative correlation by Lu et al. (1985), adopted by Li et al. (1996) and Li (1998).

Fe-shale deposits of the Datangpo and Fulu Formations would also correlate across the SCB during interglacial time. The 'Z1' pole and its corresponding paleolatitude grid would apply to all of the glaciogenic rocks under this scheme as well. Unfortunately, the  $\sim 30\text{--}40^\circ$  paleolatitudes of the lower Sinian glaciogenic deposits are neither high nor low enough to negate any of the existing models of Neoproterozoic glaciations (e.g. Harland, 1964; Williams, 1975; Meert and Van der Voo, 1994). If through future work the 'B' component could be identified confidently with the latest stages of a diachronous Nantuo glaciation, then this would severely undermine the high-obliquity hypothesis of Williams (1975).

The combined mean 'Z1' pole may carry some important implications for Sinian stratigraphy. Because the 748 Ma Liantuo paleopoles (this study) agree so well with both pre- and post-

Nantuo paleopoles of Zhang and Piper (1997), it is plausible that all of the studied lower Sinian rocks are approximately coeval; i.e. the Nantuo glacial deposits, at least in Yunnan, are not much younger than  $\sim 750$  Ma. This supports correlation of these units with a postulated 'Sturtian' or 'Rapitan' glaciation (Hambrey and Harland, 1985; Brookfield, 1994; Li et al., 1995, 1996; Khomentovsky, 1996). In addition, a  $\sim 750$  Ma age for the Nantuo Formation would appear to negate its alternative correlation with a postulated  $\sim 600$  Ma 'Marinoan' or 'Varanger' glacial episode (Chumakov, 1981; Meert and Van der Voo, 1994; Pelechaty, 1998). Note, however, that a  $\sim 600$  Ma age for the Nantuo deposits is not entirely ruled out; coincidence of the  $\sim 750$  Ma Liantuo and Nantuo poles may also be explained by an undiscovered loop or 'quasi-static' interval of the late Neoproterozoic SCB apparent polar wander path.

Further paleomagnetic studies on 700–650 Ma rocks from the SCB are required to test these possibilities.

## 6.2. Implications for ~750 Ma paleogeography

A primary paleomagnetic pole from the SCB at  $748 \pm 12$  Ma permits evaluation of several paleogeographic models of the Rodinia supercontinent. Whereas many workers prefer to reconstruct South China somewhere adjacent to Australia during Neoproterozoic time, the precise location and relative orientation are unclear. Fig. 12 shows three proposed reconstructions of the SCB against Australia, from west to east: Kirschvink (1992a), Zhang and Piper (1997), and Li et al. (1995, 1996). To test these reconstructions, the 'Z1' pole may be compared directly with new, well-dated, mid-Neoproterozoic paleomagnetic data from Australia (Wingate and Giddings, 2000).

None of the three proposed reconstructions

produces an overlap between our combined Z1 paleopole and the  $755 \pm 3$  Ma, Mundine Well dyke swarm (MDS) paleopole (Wingate and Giddings, 2000). Therefore, those reconstructions are invalid for ~750 Ma. Nonetheless, several alternative reconstructions of the SCB alongside the northwest or eastern margins of Australia are compatible with the new SCB paleomagnetic data (Fig. 13). The new models differ from their predecessors mainly in paleo-orientation, with only ~5–10° difference in paleolatitude. The displayed fits are completely adjustable in longitude, as well as in any direction within the error limits of the paleopoles (within ~4–5° for the MDS pole). Laurentia is included in Fig. 13(b) for comparative purposes; its approximate position is reconstructed according to the 755 Ma interpolated pole position of Wingate and Giddings (2000), who discuss the Australian–Laurentian paleogeographic implications extensively.

A choice of reconstruction for the SCB off the northwestern margin of the Australian craton [Fig. 13(a), model #1] has advantages and disadvantages. Cambrian faunal provinces (Burrett and Stait, 1986) and magnetostratigraphic results from the Proterozoic–Cambrian boundary (Kirschvink, 1978a,b; Fang et al., 1988/1989) and Cambrian–Ordovician boundary (Ripperdan, 1990; Ripperdan and Kirschvink, 1992) on both continents, lend credence to the notion that there was a physical connection between the two at ~500 Ma. If so, the connection could easily extend into Neoproterozoic time, when the relatively fragmentary macroscopic fossil record prohibits biogeographical comparisons. Furthermore, the orientation of the SCB in this model preserves the consistency between great-circle swathes of (generally poorly dated) late Sinian–Cambrian paleomagnetic poles from the two cratons, as noted by Zhang and Piper (1997). On the other hand, there are several major geological disparities between the SCB and the western side of Australia during the interval 600–400 Ma, summarized by Li and Powell (1999). One of these is the apparent lack of a Marinoan-equivalent glaciation in South China, as suggested by our paleomagnetic results (see above), which contrasts markedly with the extensive late-to-latest Neoproterozoic glacial

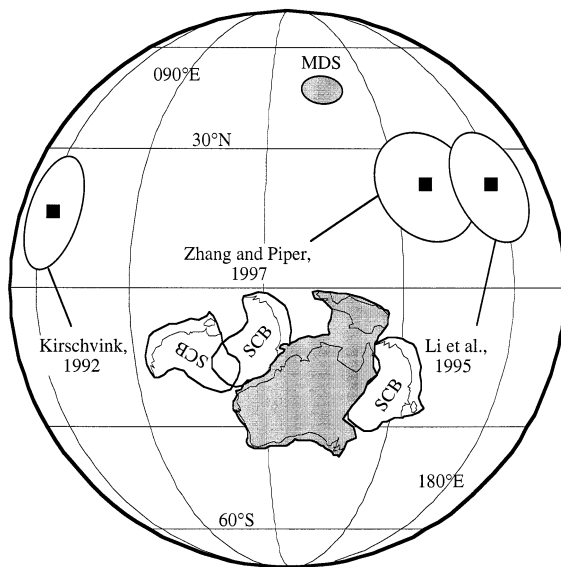


Fig. 12. Hypothesized reconstructions of the South China block (SCB) relative to Australia, and comparisons of the rotated 'Z1' pole with the  $755 \pm 3$  Ma Mundine Well dyke swarm (MDS) pole from cratonic Australia (Wingate and Giddings, 2000). Right-hand reconstruction poles from the SCB to Australia are as follows: Kirschvink (1992a)  $05.8^\circ\text{N}$ ,  $111.0^\circ\text{E}$ ,  $+162.82^\circ$ ; Zhang and Piper (1997)  $11.0^\circ\text{N}$ ,  $146.5^\circ\text{E}$ ,  $+68.5^\circ$ , and Li et al. (1995, 1996)  $21.6^\circ\text{N}$ ,  $160.0^\circ\text{E}$ ,  $+90.7^\circ$ .

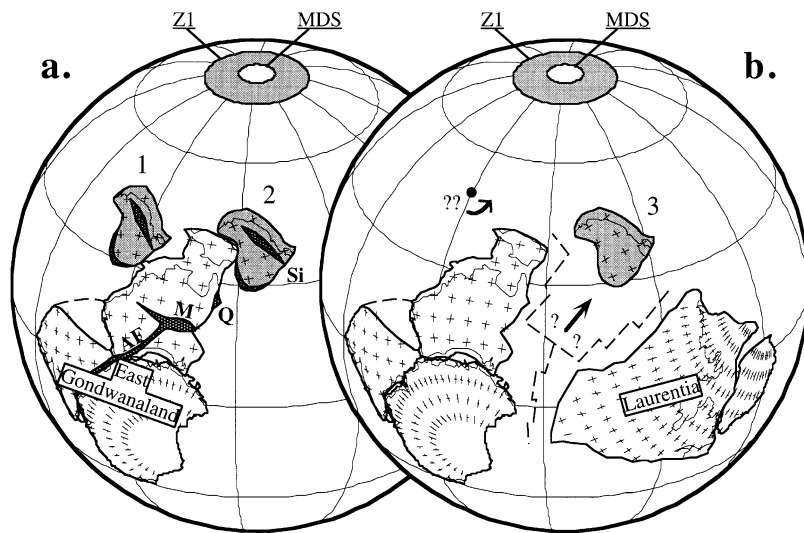


Fig. 13. Possible paleogeographic models of the SCB relative to East Gondwanaland and/or Laurentia. Orthographic projections;  $30^\circ$  grid system is defined by the  $748 \pm 12$  Ma 'Z1' pole (this study), the  $755 \pm 3$  Ma Mundine Well dyke swarm (MDS) paleomagnetic result (Wingate and Giddings, 2000), and an interpolated 755 Ma pole for Laurentia (ibid.). Note that these reconstructions are unconstrained in longitude, and continental positions may be adjusted within the error limits of the paleomagnetic studies. (a) Models #1–2, showing possible Rodinia reconstructions of the SCB immediately adjacent to the Australian craton. Regions with significant late Mesoproterozoic (1.3–1.0 Ga) tectonothermal activity are delineated: AF = Albany–Fraser belt, M = Musgrave orogen, Q = inliers in northern Queensland, Si = Sibao orogeny of southeastern China and possibly coeval belt in Sichuan Province. (b) Model #3, with Rodinia breakup preceding  $\sim 750$  Ma (cf. Wingate and Giddings, 2000). Two queried kinematic alternatives for the opening of the Pacific Ocean are indicated.

record of the Kimberley region in northwestern Australia (Plumb, 1996; Corkeron et al., 1996; Grey and Corkeron, 1998).

An alternative reconstruction of the SCB in the vicinity of Australia at  $\sim 750$  Ma is a position connected to the latter's northeast margin [Fig. 13(a), model #2]. Because Australia and Laurentia may have separated prior to  $\sim 750$  Ma (Wingate and Giddings, 2000), and assuming that no other continental blocks lay between Laurentia and the SCB, the configuration of model #2 implies rifting on the 'Cathaysia' (present southeastern) side of the SCB prior to  $\sim 750$  Ma, but rifting on the 'Qinling' (present northern) side sometime later. A rifting event between 850 and 750 Ma is relatively well-documented throughout the SCB (Li, 1998), but any subsequent Neoproterozoic or early Paleozoic rift events cannot yet be identified confidently. As an older point of comparison, however, recent structural and geochronological determinations among inliers of northern Queensland have confirmed a late Mesoproterozoic ('Grenvillian')

tectonic event (Hutton et al., 1996; Blewett and Black, 1998) that may provide a link between the 1.3–1.0 Ga Albany–Fraser–Musgrave belts in southwestern and central Australia (Black et al., 1992; Nelson et al., 1995), and regions of the SCB with similarly aged events (e.g. Sibao orogeny; Li, 1998). As noted by Li et al. (1995), these areas may constitute a once-contiguous fragment of the system of late Mesoproterozoic orogenic belts that amalgamated the Rodinia supercontinent (Hoffman, 1991).

A third possibility for reconstructing these blocks at  $\sim 750$  Ma [Fig. 13(b), model #3], is that Rodinia's fragmentation — at least around the Laurentian–Australian sector — was already completed by that time (cf. Wingate and Giddings, 2000). In that case, the discrepancies among the paleomagnetic poles shown in Fig. 12 are irrelevant to the preceding Rodinia configuration. Because longitude is unconstrained in these reconstructions, this model is not precise. However, it can be seen that model #3 is compatible with a 'missing link'

reconstruction of South China between East Gondwanaland and Laurentia, that became fragmented by  $\sim 750$  Ma. Opening of the intervening oceanic basin could have been accomplished by a three-armed spreading system with substantial transform components on either side of the SCB, manifested by NE–SW translational motion between the SCB and East Gondwanaland (cf. Li et al., 1996), but that would reconstruct the SCB in an orientation  $\sim 90^\circ$  different from the orientation originally postulated in the ‘missing link’ hypothesis (Li et al., 1995, 1996; compare with Fig. 12). Alternatively, the small ocean basin could have opened in ‘windscreen-wiper’ fashion, with an approximate Euler pole location shown. In that model, kinematically akin to the Cenozoic wrench-like rifting of the Arabian peninsula from north-eastern Africa, the ‘missing link’ reconstruction would remain viable.

To distinguish among the possible paleogeographies outlined above, more reliable Neoproterozoic paleomagnetic poles are needed from South China, Australia, and Laurentia. Paleomagnetic syntheses have already produced a plausible, but not unique, Rodinia reconstruction (Weil et al., 1998). If we wish to understand, however, the tectonic framework of the intriguing paleoclimatic and biological events of the succeeding period (Knoll and Walter, 1992), then quantitative reconstructions of the continents can only be achieved through careful paleomagnetic studies. The present database is sorely lacking in these. In particular, the SCB lacks high-quality paleomagnetic poles from the interval 700–500 Ma (Zhang and Piper, 1997); Australia lacks reliable poles for the period 725–625 Ma (Powell et al., 1993; Wingate and Giddings, 2000); and Laurentia lacks good results for the time span of 700–600 Ma (Torsvik et al., 1996). These long intervals with little or no kinematic constraints must be filled with reliable paleomagnetic data before a quantitative post-Rodinian paleogeographic framework can truly take shape.

### Acknowledgements

We thank Mao Xiaodong, Ma Guogan, Wang Chuanshang, Zhang Shuhuai, and Wang Xiaofeng

for their gracious hospitality in Yichang and assistance in the field; and Mart Idnurm, Malcolm Walter, and John Veevers for helpful suggestions to improve the manuscript. Paleomagnetic computational routines were greatly aided by the Paleomag and GMAP software packages, respectively administered by Craig Jones and Trond Torsvik. This study is supported by NSF Grant EAR94-18523 to JLK, an NSF Graduate Research Fellowship and UWA Postdoctoral Fellowship to DADE, and an ARC QEII Fellowship to ZXL. Tectonics SRC contribution # 52.

### References

- Bell, R.T., Jefferson, C.W., 1987. An hypothesis for an Australian–Canadian connection in the Late Proterozoic and the birth of the Pacific Ocean, in: Pacific Rim Congress '87. Australasian Institute of Mining and Metallurgy, pp. 39–50.
- Black, L.P., Harris, L.B., Delor, C.P., 1992. Reworking of Archaean and Early Proterozoic components during a progressive, Middle Proterozoic tectonothermal event in the Albany Mobile Belt, Western Australia. *Precambrian Res.* 59, 95–123.
- Blewett, R.S., Black, L.P., 1998. Structural and temporal framework of the Coen Region, north Queensland: implications for major tectonothermal events in east and north Australia. *Australian J. Earth Sci.* 45, 597–609.
- Brookfield, M.E., 1994. Problems in applying preservation, facies and sequence models to Sinian (Neoproterozoic) glacial sequences in Australia and Asia. *Precambrian Res.* 70, 113–143.
- Burrett, C., Stait, B., 1986. China and southeast Asia as part of the Tethyan margin of Cambro-Ordovician Gondwanaland. In: McKenzie, K.G. (Ed.), *Shallow Tethys 2: Wagga Wagga*, International Symposium on Shallow Tethys 2, 65–77.
- Butler, R.F., 1992. *Paleomagnetism: Magnetic Domains to Geologic Terranes*. Blackwell Scientific, Boston. 319 pp.
- Chumakov, N.M., 1981. Upper Proterozoic glaciogenic rocks and their stratigraphic significance. *Precambrian Res.* 15, 373–395.
- Corkeron, M., Grey, K., Li, Z.X., Powell, C.McA., 1996. Neoproterozoic glacial episodes in the Kimberley region, north-western Australia. *Abstr. Geol. Soc. Australia* 41, 97.
- Crowell, J.C., 1983. Ice ages recorded on Gondwanan continents. *Trans. Geol. Soc. South Africa* 86, 237–262.
- Ding, L., Li, Y., Hu, X., Xiao, Y., Su, C., Huang, J., 1996. Sinian Miaohu Biota. Geological Publishing House, Beijing. 221 pp.
- Eisbacher, G.H., 1985. Late Proterozoic rifting, glacial sedimentation, and sedimentary cycles in the light of Winder-

- mere deposition, Western Canada. *Palaeogeog. Palaeoclimatol. Palaeoecol.* 51, 231–254.
- Embleton, B.J.J., Williams, G.E., 1986. Low palaeolatitude of deposition for late Precambrian periglacial varvites in South Australia: implications for palaeoclimatology. *Earth Planet. Sci. Lett.* 79, 419–430.
- Enkin, R.J., Yang, Z.Y., Chen, Y., Courtillot, V., 1992. Palaeomagnetic constraints on the geodynamic history of China from the Permian to the present. *J. Geophys. Res.* 97, 13953–13989.
- Evans, D.A., 1997. Paleomagnetic and geochronologic constraints upon the Neoproterozoic climatic paradox: a global update. *Geol. Soc. Am. Abstr. Progr.* 29 (6), 195.
- Evans, D.A., 1998. I. Neoproterozoic–Paleozoic supercontinental tectonics and true polar wander, II. Temporal and spatial distributions of Proterozoic glaciations. Ph.D. Thesis, California Institute of Technology, 326 pp.
- Fang, W., Van der Voo, R., Liang, Q.Z., 1988/1989. Reconnaissance magnetostratigraphy of the Precambrian–Cambrian boundary section at Meishucun, southwest China. *Cuadernos de Geologia Iberica* 12, 205–222.
- Fang, W., Van der Voo, R., Liang, Q., 1990. Ordovician paleomagnetism of eastern Yunnan, China. *Geophys. Res. Lett.* 17, 953–956.
- Fisher, R.A., 1953. Dispersion on a sphere. *Proc. Roy. Soc. London, Ser. A* 217, 295–305.
- Grabau, A.W., 1922. The Sinian System. *Bull. Geol. Soc. China* 1, 44–88.
- Grey, K., Corkeron, M., 1998. Late Neoproterozoic stromatolites in glacial successions of the Kimberley region, Western Australia: evidence for a younger Marinoan glaciation. *Precambrian Res.* 92, 65–87.
- Hambrey, M.J., Harland, W.B., 1985. The Late Proterozoic glacial era. *Palaeogeogr. Palaeoclimatol. Palaeoecol.* 51, 255–272.
- Harland, W.B., 1964. Critical evidence for a great infra-Cambrian glaciation. *Geol. Rundsch.* 54, 45–61.
- Hoffman, P.F., 1991. Did the breakout of Laurentia turn Gondwanaland inside-out? *Science* 252, 1409–1412.
- Hoffman, P.F., Kaufman, A.J., Halverson, G.P., Schrag, D.P., 1998. A Neoproterozoic snowball Earth. *Science* 281, 1342–1346.
- Hutton, L., Fanning, C.M., Garrad, P., 1996. Grenvillian age magmatic and metamorphic event in the Cape River area, North Queensland: significance for late Mesoproterozoic continental reconstructions. *Geol. Soc. Australia Abstr.* 41, 209.
- Kent, D.V., Smethurst, M.A., 1998. Shallow bias of paleomagnetic inclinations in the Paleozoic and Precambrian. *Earth Planet. Sci. Lett.* 160, 391–402.
- Kent, D.V., Zeng, X., Zhang, W.Y., Opdyke, N.D., 1987. Widespread late Mesozoic to Recent remagnetization of Paleozoic and lower Triassic sedimentary rocks from South China. *Tectonophysics* 139, 133–143.
- Khomentovsky, V.V., 1996. Sinian System in China and its analogs in Siberia. *Russian Geol. Geophys.* 37, 129–144.
- Kirschvink, J.L., 1978a. The Precambrian–Cambrian boundary problem: magnetostratigraphy of the Amadeus Basin, Central Australia. *Geol. Mag.* 115, 139–150.
- Kirschvink, J.L., 1978b. The Precambrian–Cambrian boundary problem: Paleomagnetic directions from the Amadeus Basin, Central Australia. *Earth Planet. Sci. Lett.* 40, 91–100.
- Kirschvink, J.L., 1980. The least-squares line and plane and the analysis of palaeomagnetic data. *Geophys. J. Roy. Astronom. Soc.* 62, 699–718.
- Kirschvink, J.L., 1992a. A paleogeographic model for Vendian and Cambrian time. In: Schopf, J.W., Klein, C. (Eds.), *The Proterozoic Biosphere: A Multidisciplinary Study*. Cambridge University Press, Cambridge, pp. 569–581.
- Kirschvink, J.L., 1992b. Late Proterozoic low-latitude global glaciation: the snowball Earth. In: Schopf, J.W., Klein, C. (Eds.), *The Proterozoic Biosphere: A Multidisciplinary Study*. Cambridge University Press, Cambridge, pp. 51–52.
- Klimetz, M.P., 1983. Speculations on the Mesozoic plate tectonic evolution of eastern China. *Tectonics* 2, 139–166.
- Knoll, A.H., Walter, M.R., 1992. Latest Proterozoic stratigraphy and Earth history. *Nature* 356, 673–678.
- Li, P., Liu, C., 1979. Paleomagnetic study of the Sinian System from eastern gorge districts of the Yangtze River. *Acta Geophys. Sinica* 22, 281–288. In Chinese with English abstract.
- Li, Z.X., Powell, C.McA., 1999. Palaeomagnetic study of Neoproterozoic glacial rocks of the Yangzi Block: palaeolatitude and configuration of South China in the late Proterozoic Supercontinent: Discussion. *Precambrian Res.* 94, 1–5.
- Li, Z.X., 1988. Palaeozoic palaeomagnetism of Australia and South China. Ph.D. Thesis, Macquarie University, 178 pp.
- Li, Z.X., 1998. Tectonic history of the major East Asian lithospheric blocks since the mid-Proterozoic: A synthesis. *Mantle Dynamics and Plate Interactions in East Asia*, Flower, M.F.J., Chung, S.-L., Lo, C.-H., Lee, T.-Y. (Eds.), *AGU Geodynam. Ser.* 27, 221–243.
- Li, Z.X., Zhang, L., Powell, C.McA., 1995. South China in Rodinia: part of the missing link between Australia–East Antarctica and Laurentia? *Geology* 23, 407–410.
- Li, Z.X., Zhang, L., Powell, C.McA., 1996. Positions of the East Asian cratons in the Neoproterozoic supercontinent Rodinia. *Australian J. Earth Sci.* 43, 593–604.
- Liao, S.-F., 1981. Sinian glacial deposits of Guizhou Province, China. In: Hambrey, M.J., Harland, W.B. (Eds.), *Earth's Pre-Pleistocene Glacial Record*. Cambridge University Press, Cambridge, pp. 414–423.
- Liu, C., Feng, H., 1965. Alternating field demagnetization study on lower Sinian sandstones in Hsiuning District, Anhwei Province. *Acta Geophys. Sinica* 14, 173–180. In Chinese with English abstract.
- Liu, C., Liu, H.S., 1965. Several paleomagnetic results from the Sinian in China. *Sci. Geol. Sinica* 1, 77–79. In Chinese.
- Lu, S., Ma, G., Gao, Z., Lin, W., 1985. Sinian ice ages and glacial sedimentary facies-areas in China. *Precambrian Res.* 29, 53–63.
- Ma, G., Lee, H., Zhang, Z., 1984. An investigation of the age limits of the Sinian System in South China. *Bull. Yichang Inst. Geol. Miner. Res., Chinese Acad. Geol. Sci.* 8, 1–29. In Chinese with English abstract.

- McFadden, P.L., McElhinny, M.W., 1988. The combined analysis of remagnetization circles and direct observations in palaeomagnetism. *Earth Planet. Sci. Lett.* 87, 161–172.
- McFadden, P.L., McElhinny, M.W., 1990. Classification of the reversal test in palaeomagnetism. *Geophys. J. Int.* 103, 725–729.
- Meert, J.G., Van der Voo, R., 1994. The Neoproterozoic (1000–540 Ma) glacial intervals: no more snowball earth? *Earth Planet. Sci. Lett.* 123, 1–13.
- Moore, E., 1991. Southwest U.S.–East Antarctic (SWEAT) connection: a hypothesis. *Geology* 19, 425–428.
- Nelson, D.R., Myers, J.S., Nutman, A.P., 1995. Chronology and evolution of the Middle Proterozoic Albany–Fraser Orogen, Western Australia. *Australian J. Earth Sci.* 42, 481–495.
- Onstott, T.C., 1980. Application of the Bingham distribution function in paleomagnetic studies. *J. Geophys. Res.* 85, 1500–1510.
- Opdyke, N.D., Huang, K., Xu, G., Zhang, W.Y., Kent, D.V., 1986. Paleomagnetic results from the Triassic of Yangtze Platform. *J. Geophys. Res.* 91, 9553–9568.
- Pelechaty, S.M., 1998. Integrated chronostratigraphy of the Vendian System of Siberia: implications for a global stratigraphy. *J. Geol. Soc. London* 155, 957–973.
- Plumb, K.A., 1996. Revised correlation of Neoproterozoic glacial successions from the Kimberley region, northwestern Australia. *Abstr. Geol. Soc. Australia* 41, 344.
- Powell, C.McA., Li, Z.X., McElhinny, M.W., Meert, J.G., Park, J.K., 1993. Paleomagnetic constraints on timing of the Neoproterozoic breakup of Rodinia and the Cambrian formation of Gondwana. *Geology* 21, 889–892.
- Ripperdan, R.L., 1990. Magnetostratigraphic investigations of the lower Paleozoic system boundaries and associated paleogeographic implications. Ph.D. Thesis, California Institute of Technology, 195 pp.
- Ripperdan, R.L., Kirschvink, J.L., 1992. Paleomagnetic results from the Cambrian–Ordovician boundary section at Black Mountain, Georgina Basin, western Queensland, Australia. In: Webby, B.D., Laurie, J.R. (Eds.), *Global Perspectives on Ordovician Geology*. Balkema, Rotterdam, pp. 93–103.
- Schermerhorn, L.J.G., 1974. Late Precambrian mixtites: glacial and/or nonglacial? *Am. J. Sci.* 274, 673–824.
- Sohl, L.E., Christie-Blick, N., Kent, D.V., 1999. Paleomagnetic polarity reversals in Marinoan (ca. 600 Ma) glacial deposits of Australia: implications for the duration of low-latitude glaciation in Neoproterozoic time. *Geol. Soc. Am. Bull.* 111, 1120–1139.
- Torsvik, T.H., Smethurst, M.A., Meert, J.G., Van der Voo, R., McKerrow, W.S., Brasier, M.D., Sturt, B.A., Walderhaug, H.J., 1996. Continental break-up and collision in the Neoproterozoic and Palaeozoic — A tale of Baltica and Laurentia. *Earth Sci. Rev.* 40, 229–258.
- Van der Voo, R., 1990. The reliability of paleomagnetic data. *Tectonophysics* 184, 1–9.
- Van der Voo, R., 1993. *Paleomagnetism of the Atlantic, Tethys and Iapetus Oceans*. Cambridge University Press, Cambridge. 411 pp.
- Wang, H., 1986. The Sinian System. In: Yang, Z., Cheng, Y., Wang, H. (Eds.), *The Geology of China*. Clarendon Press, Oxford, pp. 50–63.
- Wang, Y., Lu, S., Gao, Z., Lin, W., Ma, G., 1981. Sinian tillites of China. In: Hambrey, M.J., Harland, W.B. (Eds.), *Earth's Pre-Pleistocene Glacial Record*. Cambridge University Press, Cambridge, pp. 386–401.
- Wang, X., Erdtmann, B.D., Mao, X., et al., 1996. Geology of the Yangtze Gorges area. 30th Int. Geol. Congress Field Trip Guide T106/T340. Geological Publishing House, Beijing. 73 pp.
- Weil, A.B., Van der Voo, R., MacNiocail, C., Meert, J.G., 1998. The Proterozoic supercontinent Rodinia: paleomagnetically derived reconstructions for 1100 to 800 Ma. *Earth Planet. Sci. Lett.* 154, 13–24.
- Williams, G.E., 1975. Late Precambrian glacial climate and the Earth's obliquity. *Geol. Mag.* 112, 441–465.
- Williams, G.E., Schmidt, P.W., Embleton, B.J.J., 1995. Comment on 'The Neoproterozoic (1000–540 Ma) glacial intervals: No more snowball earth?' by J.G. Meert and R. Van der Voo. *Earth Planet. Sci. Lett.* 131, 115–122.
- Wingate, M.T.D., Giddings, J.W., 2000. Age and paleomagnetism of the Mundine Well dyke swarm, Western Australia: implications for an Australia–Laurentia connection at 755 Ma. *Precambrian Res.* 100, 335–357.
- Zhang, H.M., 1998. Preliminary Proterozoic apparent polar wander paths for the South China Block and their tectonic implications. *Canadian J. Earth Sci.* 35, 302–320.
- Zhang, Q.R., Piper, J.D.A., 1997. Palaeomagnetic study of Neoproterozoic glacial rocks of the Yangzi Block: palaeolatitude and configuration of South China in the late Proterozoic Supercontinent. *Precambrian Res.* 85, 173–199.
- Zhang, H.M., Zhang, W.Z., 1985. Palaeomagnetic data, Late Precambrian magnetostratigraphy and tectonic evolution of eastern China. *Precambrian Res.* 29, 65–75.
- Zhang, H.M., Zhang, W.Z., Li, P., 1982. Paleomagnetism of the Sinian System of eastern Yangzi gorges in China. *Bull. Tianjin Inst. Geol. Min. Res.* 6, 57–68.
- Zhang, H.M., Zhang, W.Z., Elston, D.P., 1991. Palaeomagnetism of Middle and Late Proterozoic Dagushi Group and Huashan Group, and Sinian System, Jingshan County, Hubei Province, South China. *Bull. Tianjin Inst. Geol. Min. Res.* 25, 63–78. in Chinese with English abstract.
- Zhao, X., Coe, R.S., Gilder, S.A., Frost, G.M., 1996. Palaeomagnetic constraints on the palaeogeography of China: implications for Gondwanaland. *Australian J. Earth Sci.* 43, 643–672.